

Research Article

Next-Generation Sequencing Panel Analysis of Clinically Relevant Mutations in Circulating Cell-Free DNA from Patients with Gestational Trophoblastic Neoplasia: A Pilot Study

Lingxiao Luo,^{1,2} Ling Lin,³ Xiaoyan Zhang,^{1,2} Qingqing Cai,^{1,2} Hongbo Zhao,^{1,2} Congjian Xu ^{1,2} and Qing Cong ^{1,2}

¹Obstetrics and Gynecology Hospital of Fudan University, Shanghai 200011, China

²Shanghai Key Laboratory of Female Reproductive Endocrine Related Diseases, Fudan University, Shanghai 200011, China

³Institutes of Biomedical Sciences of Shanghai Medical School, Fudan University, Shanghai 200032, China

Correspondence should be addressed to Congjian Xu; xucongjian@fudan.edu.cn and Qing Cong; jennifercong@163.com

Received 27 September 2019; Revised 7 December 2019; Accepted 10 December 2019; Published 8 January 2020

Academic Editor: Salah Aref

Copyright © 2020 Lingxiao Luo et al. This is an open access article distributed under the Creative Commons Attribution License, which permits unrestricted use, distribution, and reproduction in any medium, provided the original work is properly cited.

Gestational trophoblastic neoplasia (GTN) originates from placental tissue and exhibits the potential for invasion and metastasis. Gene alterations in GTN have not been extensively studied because of a lack of qualified tumor specimens after chemotherapy. GTN has a rapid growth rate and is highly metastatic, which makes circulating tumor DNA (ctDNA) sequencing a promising modality for gene profiling. Accordingly, in this study, we performed targeted next-generation sequencing (NGS) of 559 tumor-associated genes using circulating cell-free DNA (cfDNA) collected prior to chemotherapy from 11 patients with GTN. All sequenced genes were associated with oncogenesis, progression, and targeted therapy. The average cfDNA level was 0.43 ± 0.22 ng/ μ L. Significant correlations were found between cfDNA concentration and maximum lesion diameter ($r = 0.625$, $p = 0.040$) and time for human chorionic gonadotropin beta subunit (β -HCG) recovering to normal level ($r = 0.609$, $p = 0.047$). There were no significant correlations between cfDNA concentrations and β -HCG expression level or lung metastasis. ctDNA mutations were detected in all patients, and 73 mutant genes were detected in 11 patients. *BMPRIA* (27.3%), *LRP1B* (27.3%), *ERCC4* (18.2%), *FGF14* (18.2%), *HSP90AA1* (18.2%), *KAT6A* (18.2%), *KMT2D* (18.2%), *MAP3K1* (18.2%), *RANBP2* (18.2%), and *ZNF217* (18.2%) mutations were detected as overlapping mutations. The mRNA and protein levels of bone morphogenetic protein receptor type 1A were significantly downregulated in human JAR and JEG-3 choriocarcinoma cells ($p < 0.0001$), whereas mRNA and protein levels of mitogen-activated protein kinase kinase 1 were upregulated in these two cell lines ($p = 0.0128$, $p = 0.0012$, respectively). These genes may play important roles in GTN initiation and progression and may be candidate targets for GTN treatment. These findings suggested that cfDNA levels could provide potential assessment value in disease severity of GTN and that ctDNA sequencing was a promising approach for identifying gene mutations in GTN.

1. Introduction

Gestational trophoblastic neoplasia (GTN) is a cancer that originates from placental tissue and exhibits the potential for invasion and widespread metastasis. GTN includes invasive moles, choriocarcinoma, placental site trophoblastic tumors, and epithelioid trophoblastic tumor, encompassing lesions that originate in the chorionic villi and the extravillous trophoblast; these lesions exhibit different degrees of proliferation, invasion, and dissemination [1, 2]. GTN generally

spreads to the lungs, liver, central nervous system, and vagina. Accordingly, detection of metastasis is essential for evaluating disease progression [3]. GTN secretes human chorionic gonadotropin beta subunit (β -HCG), which serves as a useful biomarker, contributing to diagnosis, monitoring of therapeutic response, early detection of relapse, and assessment of cure [4, 5].

GTN is highly vascular, and biopsy is associated with a high risk of hemorrhage; thus, histological diagnosis is not necessary for treatment. However, chemotherapy is a highly

effective, first-line treatment for GTN. Most women can be cured by chemotherapy without undergoing surgery, and surgery is often only performed when chemotherapy resistance is encountered. Tumors are often destroyed by chemotherapy and cannot be used for genetic research. Therefore, gene alterations of GTN have not been extensively studied.

With the development of precision medicine, liquid biopsy has emerged as a promising, noninvasive method for analysis of circulating tumor-derived material. Liquid biopsies, including tumor circulum, cell-free DNA (cfDNA), circulating tumor DNA (ctDNA), and circulating tumor cells, represent an innovative tool in precision oncology to overcome current limitations associated with tissue biopsies [6]. GTN has a rapid growth rate and is highly metastatic, showing early hematogenous spread. Thus, ctDNA sequencing may be a promising modality for genomic profiling and a viable tool for detecting more sensitive and specific biomarkers for clinical utility. ctDNA sequencing has been reported to have potential for disease monitoring, minimal residual disease detection, and therapeutic efficacy analysis in multiple different types of cancer [7–11]. However, few studies have reported cfDNA in gestational trophoblastic tumors.

Therefore, in this study, we investigated serum levels and gene alterations of targeted cfDNA in GTN, with the goal of elucidating the potential clinical and etiological roles of cfDNA in GTN.

2. Materials and Methods

2.1. Patients and Clinical Characteristics. Patients with GTN who met the inclusion criteria were enrolled in the Obstetrics and Gynecology Hospital of Fudan University from September 2017 to September 2018. Patients were included in the study according to the following criteria: diagnosed with GTN, according to the systematization of the diagnosis and GTN staging proposed by FIGO [12]; had not undergone chemotherapy; did not have any other tumorous disease or medical comorbidities; did not have any injury history or had not received any hormone therapy within 1 year prior to enrollment; and could be followed-up. Our project was approved by the Medical Ethics Committee of the Obstetrics and Gynecology Hospital of Fudan University, and all enrolled patients signed a consent form.

2.2. Reagents and Instruments. Reagents included anti-glyceraldehyde 3-phosphate dehydrogenase (GAPDH) antibody (cat. no. KC-5G4; Aksomics, Shanghai, China), antibody morphogenetic protein receptor type 1A (BMPRI1A) antibody (cat. no. 12702-1-AP; Proteintech, IL, USA), antimitogen-activated protein kinase kinase 1 (MAP3K1) antibody (cat. no. 19970-1-AP; Proteintech, IL, USA), Magnetic Serum/Plasma DNA Maxi Kit (Tiangen, Beijing, China), TRIzol reagent (Invitrogen, CA, USA), PrimeScript RT kit, and SYBR Premix Ex Taq II (Takara, Shiga, Japan). Instruments included an optical microscope, an inverted microscope and imaging system (Olympus,

Tokyo, Japan), and an ABI 7900 real-time PCR system (Applied Biosystems, MA, USA).

2.3. Plasma Collection and Preparation. Ten milliliters of peripheral blood was collected in Cell Free DNA BCT before chemotherapy from patients with gestational trophoblastic tumors and then separated by centrifugation at $1600 \times g$ for 10 min at 4°C . The plasma layer was separated, and an additional centrifugation step at $16,000 \times g$ for 10 min was included. Plasma was stored at -80°C until analysis.

2.4. cfDNA Preparation. cfDNA was prepared from 3 mL plasma according to the manufacturer's instructions using a Magnetic Serum/Plasma DNA Maxi Kit (Tiangen). cfDNA was quantified using an Agilent 2100 Bioanalyzer (Agilent, CA, USA). We used a targeted NGS panel (MyGenostics, Beijing, China) in this study, which included 559 genes reported to be associated with oncogenesis, progression, and targeted therapy (Supplementary Table 1). Whole exome sequencing of the 559 genes was performed to identify gene alterations in ctDNA from patients with GTN with a target region sequencing depth of more than 500x. DNA from paired peripheral blood mononuclear cells of the same patient was sequenced as the germline control.

2.5. Cell Culture. The human choriocarcinoma cell lines JEG-3 and JAR were obtained from the cell bank at the Chinese Academy of Sciences (Shanghai, China). The human trophoblast cell line HTR8/sev8 was purchased from JENNICO Biological Technology (Guangzhou, China). These cell lines were obtained within 6 months before being used in this study and were authenticated by short tandem repeat validation analysis. HTR8/sev8 cells were cultured in 1640 complete medium, and JEG-3 and JAR cells were cultured in Dulbecco's modified Eagle's medium (DMEM); both 1640 complete medium and DMEM complete medium were supplemented with 10% fetal bovine serum (Gibco, CA, USA), 100 IU/mL penicillin G, and 100 mg/mL streptomycin sulfate (Gibco).

2.6. Real-Time Quantitative Polymerase Chain Reaction (qPCR). Total RNA was extracted using TRIzol reagent (Invitrogen) according to the manufacturer's instructions, followed by reverse transcription (RT) PCR using a PrimeScript RT kit (Takara) to generate cDNA. qPCR assay for multiple genes was then performed with SYBR Premix Ex Taq II (Takara) on an ABI 7900 real-time PCR system (Applied Biosystems). The *GAPDH* gene was used as a housekeeping gene. To ensure the qPCR quality, two or three primer pairs were designed for all amplification segments, but only one pair was used in the final test. Melting-curve analyses were performed for all primers. To normalize cycle threshold (Ct) values obtained for each gene. All qPCR assays were repeated three times. The primers used for the detection of *BMPRI1A*, *MAP3K1*, *HSP90AA1*, *ZNF217*, *RANBP2*, and *GAPDH* are described in Table 1.

TABLE 1: Clinical characteristics of the 11 GTN patients.

Patients	Age	Antecedent pregnancy	Interval from index pregnancy (months)	Distant metastasis (number)	Maximum lesion diameter (cm)	Plasma HCG level (U/L)	Chemotherapy regimens*	Surgery [#]	Pathologic results	Diagnosis	Time for β -HCG recovering to normal level (days)	cfDNA concentration (ng/ μ L)
P1	48	Mole	1	Lung (6)	3.0	33740	EMA-CO	TLH	Invasive mole	GTN III:6	63	0.181
P2	52	Mole	1	Lung (6)	6.6	>272600	EMA-CO	TLH and BSO	Invasive mole	GTN III:9	112	0.928
P3	40	Mole	>12	No	8.2	1622	EMA-CO	Uterine wedge resection	Choriocarcinoma	GTN I:8	80	0.522
P4	25	Mole	4	No	3.0	4209	Actinomycin D	Uterine wedge resection	Choriocarcinoma	GTN I:3	63	0.477
P5	34	Mole	3	No	3.1	170672	EMA-CO	No	None	GTN I:5	60	0.28
P6	26	Mole	1	Lung (1)	7.0	5036	Actinomycin D	No	None	GTN III:4	76	0.596
P7	25	Mole	1	Lung (7)	4.2	12730	EMA-CO	No	None	GTN III:5	69	0.199
P8	24	Mole	1	Lung (2)	3.9	12498	EMA-CO	No	None	GTN III:4	89	0.419
P9	43	Abortion	3	No	5.0	121750	EMA-CO	TLH	Choriocarcinoma	GTN I:8	111	0.517
P10	30	Abortion	2	Lung (4)	4.2	18030	EMA-CO	D&C	Choriocarcinoma	GTN III:5	83	0.211
P11	28	Mole	4	No	6.1	15957	EMA-CO	Uterine wedge resection	Invasive mole	GTN I:5	49	0.403

*EMA-CO: etoposide, methotrexate, actinomycin D, cyclophosphamide, vincristine. [#]TLH: total laparoscopic hysterectomy; BSO: bilateral salpingo-oophorectomy; D&C: dilatation and curettage.

2.7. Western Blotting. JEG-3, JAR, and HTR8/sev8 cells were lysed in sodium dodecyl sulfate (SDS) lysis buffer (50 mM Tris-HCl, pH 6.8, 2% SDS, 10% glycerol, 1 mM phenylmethylsulfonylfluoride, and 1 mM Na_3VO_4). Equal amounts of total protein were separated by SDS-polyacrylamide gel electrophoresis and then transferred to polyvinylidene fluoride membranes (Merck Millipore, MA, USA). After blocking with 5% nonfat milk for 2 h, the membranes were incubated with primary antibodies at 4°C overnight, washed, and incubated with corresponding secondary antibodies at room temperature for 60 min. The protein bands of interest were visualized by fluorography using an enhanced chemiluminescence system (Pierce Protein Biology, IL, USA). BMPR1A and MAP3K1 expression levels were quantified and normalized to the expression of the loading control (GAPDH). Means \pm standard deviations of triplicate experiments were plotted by GraphPad Prism software (version 8.0).

2.8. Statistical Analysis. Each experiment was repeated at least three times. Statistical analyses were performed using SPSS 23.0 (IBM Corporation, NY, USA) and Prism 8.0 (GraphPad Software, CA, USA). Data are presented as the means \pm standard deviations. Statistical analyses were performed with Pearson analysis and Student's *t* tests, and results with *p* values of less than 0.05 were considered significant.

3. Results

3.1. Clinical Features and cfDNA Concentrations. Eleven patients (aged 24–48 years, range: 34.1 ± 10.1 years) were enrolled in this study. Clinical characteristics are demonstrated in Table 1. Among them, 9 of 11 patients had an antecedent molar pregnancy. Pathologic results of surgical specimens identified 4 cases of choriocarcinoma. According to the International Federation of Gynecology and Obstetrics (FIGO) prognosis scoring system, eight of the eleven GTN patients were low risk (8/11, 72.7%), and three were high risk (3/11, 27.3%). Among them, patients with low-risk GTN (FIGO risk score 0–4) was treated with the single agent actinomycin D protocols. We reduced the threshold for the use of multiple agent chemotherapy in these patients with higher FIGO risk score (5–6) because of the increased risk of resistance to single agent chemotherapy. The cure rate of treatment was 100%, and all the patients' β -HCG concentrations recovered to normal level within 4 months (77.7 ± 20.2 days).

We detected the cfDNA levels of all patients with GTN. The average cfDNA level was 0.43 ± 0.22 ng/ μ L. The distribution of the maximum lesion diameter as well as the time for HCG recovery were checked using SPSS Statistics software (version 20). The Kolmogorov–Smirnov Sig. values both equaled 0.2, which was greater than 0.05; thus, the maximum lesion diameter and HCG recovery time were normally distributed. Pearson correlation analysis showed that there were correlations between the concentration of cfDNA and the maximum diameter of lesions ($r=0.6254$,

$p = 0.040$; Figure 1(a)) and the time for β -HCG recovery to normal levels ($r=0.6095$, $p = 0.047$; Figure 1(b)). However, the distribution of β -HCG levels was not normal because the Kolmogorov–Smirnov Sig. value equaled 0.001 (Supplementary Table 2). The relationship between β -HCG levels and cfDNA concentrations was evaluated using Spearman's correlation analysis. The correlation between plasma β -HCG levels and cfDNA concentrations was low ($r=-0.1545$), and the *p* value indicated a lack of significance ($p = 0.654$). Moreover, Student's *t*-tests showed that there were no significant correlations between the presence of lung metastasis and the concentration of cfDNA ($p = 0.90$) or patient age ($p = 0.24$; Figures 1(d) & 1(e)).

3.2. Gene Mutation Analysis Based on Next-Generation Sequencing (NGS) Panel Analysis of Clinically Relevant Mutations in cfDNA. ctDNA mutations were detected in all patients, and 73 mutant genes were detected in 11 patients. Eleven genes, including BMPR1A (3/11, 27.3%), low-density lipoprotein receptor-related protein 1B (LRP1B; 3/11, 27.3%), excision repair cross-complementing 4 (ERCC4; 2/11, 18.2%), fibroblast growth factor 14 (FGF14; 2/11, 18.2%), heat shock protein 90 alpha family class A member 1 (HSP90AA1; 2/11, 18.2%), lysine acetyltransferase 6A (KAT6A; 2/11, 18.2%), lysine methyltransferase 2D (KMT2D; 2/11, 18.2%), MAP3K1 (2/11, 18.2%), RAN binding protein 2 (RANBP2; 2/11, 18.2%), and Zinc finger protein 217 (ZNF217; 2/11, 18.2%), showed overlapping mutations (Figure 2, Table 2).

3.3. Expression of Overlapping Mutations in Cell Lines. The mRNA levels of BMPR1A were decreased in human JAR and JEG-3 choriocarcinoma cells ($p < 0.0001$), whereas the protein levels of BMPR1A were decreased slightly ($p > 0.05$). MAP3K1 mRNA levels were increased in JAR and JEG-3 cell lines ($p = 0.0128$, $p = 0.0012$, respectively), and MAP3K1 protein levels were also upregulated significantly ($p = 0.0056$, $p = 0.0006$, respectively). The mRNA levels of RANBP2 and ZNF217 were higher in JAR cell lines than in HTR8 cells ($p = 0.0008$, $p = 0.0026$, respectively); however, there were no significant differences between JEG-3 and HTR8 cells. There were no significant differences in HSP90AA1 mRNA expression among these three cell lines (Figures 3 and 4).

4. Discussion

GTN mainly spreads by hematogenous dissemination. Therefore, in this study, we evaluated cfDNA, which provided complementary clinically relevant information for GTN. cfDNA consists of nucleic acids released from necrotic and apoptotic cells into blood circulation and is thought to be derived from both healthy and cancer cells [13]. cfDNA levels are higher in patients with cancer (0–1,000 mg/mL) than in healthy individuals (0–100 ng/mL). cfDNA analysis has been reported to have potential clinical utility in disease diagnosis and monitoring as well as early indicators of therapeutic efficacy in multiple cancer types [14–17].

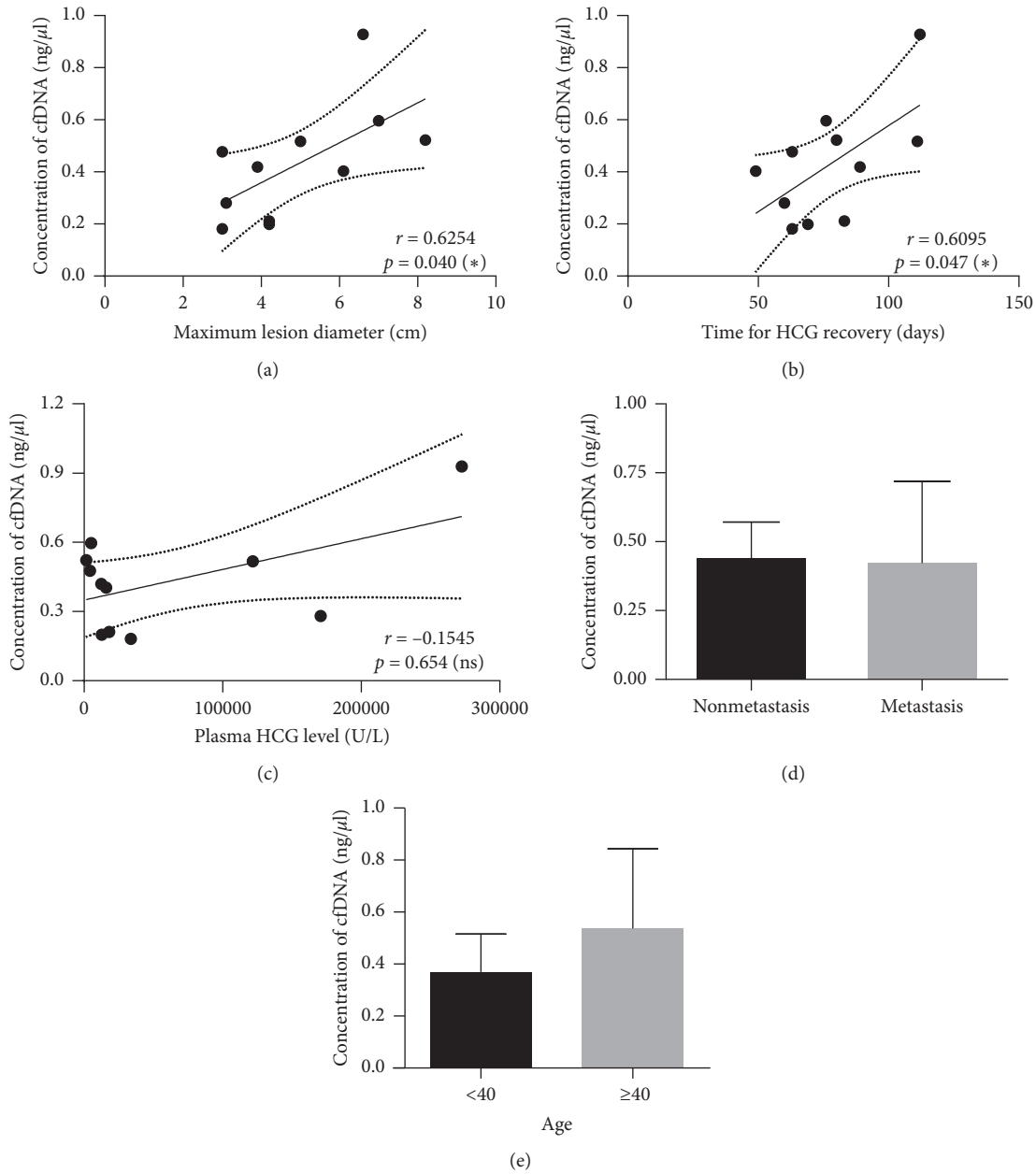


FIGURE 1: Relativity of clinical characteristics and the concentration of cfDNA. (a) Correlation of maximum lesion diameter and the concentration of cfDNA; (b) correlation of the time for β -HCG recovering to normal level and the concentration of cfDNA; (c) correlation of plasma HCG level and cfDNA concentration; (d) correlation of distant metastasis and cfDNA concentration ($p = 0.90$); (e) correlation of age and cfDNA concentration ($p = 0.24$).

However, few studies have investigated cfDNA in GTN. For example, Openshaw et al. reported that the presence of ctDNA was associated with serum hCG levels in women with GTN [18]. Additionally, in our study, we found that the maximum lesion diameter and the time for β -HCG recovery to normal levels were positively correlated with the levels of cfDNA in patients with GTN; thus, these factors may be used to reflect the tumor burden and evaluate the condition and prognosis of GTN, consistent with previous studies [19–21]. During tumorigenesis, apoptotic and necrotic tumor cells are engulfed by immune-related cells, such as monocytes and macrophages, thus releasing a large number of DNA

fragments, which can increase the concentration of cfDNA. In addition, cfDNA levels may also increase because of the lysis of white blood cells, resulting in release of germline DNA.

We detected mutations in all pretreatment plasma samples in the 11 patients in this study, including 10 key overlapping mutant genes (*BMP1A*, *LRP1B*, *ERCC4*, *FGF14*, *HSP90AA1*, *KAT6A*, *KMT2D*, *MAP3K1*, *RANBP2*, and *ZNF217*). These genes, particularly *MAP3K1* and *BMP1A*, may be candidate genes in GTN initiation and progression, and could be targeted in the development of novel treatments for GTN. Sekiya et al. [22] examined the

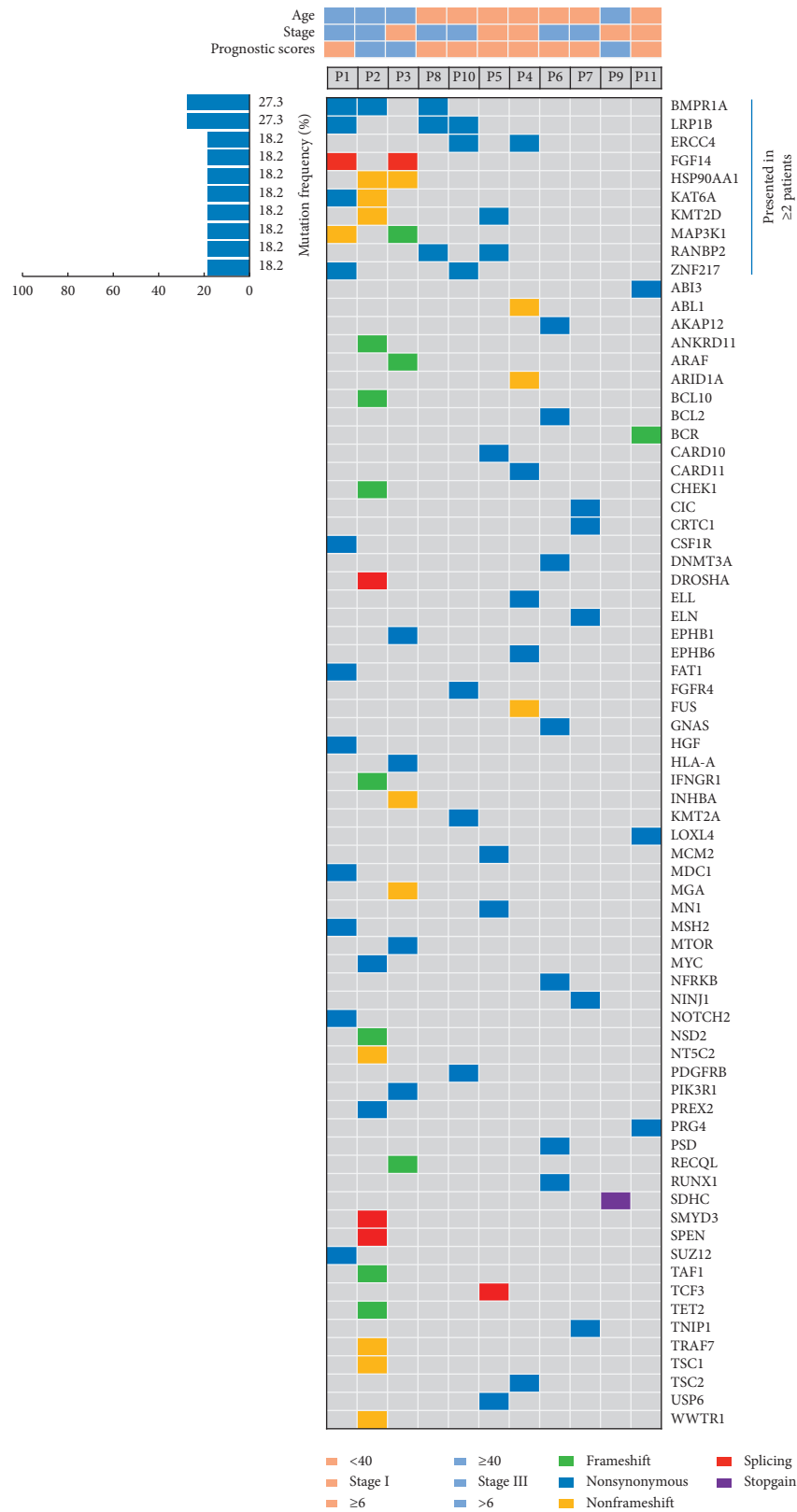


FIGURE 2: ctDNA sequencing results of GTN patients.

expression of nuclear factor- κ B family proteins in normal placenta and choriocarcinoma cell lines; their results suggested that c-Rel may play a role in promoting the invasion

of choriocarcinoma cells through phosphatidylinositol 3-kinase (PI3K)/AKT signaling. Additionally, Mello et al. [23] also revealed the involvement of phosphatase and tensin

TABLE 2: Details of overlapping mutations.

No.	Gene	Transcript	Patients	Exons	Nucleotide variation	Type
1	BMPRI1A	NM_004329	P1	Exon10	c.1001 T > C	SNV
			P2	Exon10	c.1001 T > C	SNV
			P8	Exon10	c.1001 T > C	SNV
2	LRP1B	NM_018557	P1	Exon39	c.6221 A > C	SNV
			P9	Exon43	c.7034 T > G	SNV
			P10	Exon39	c.6221 A > C	SNV
3	ERCC4	NM_005236	P4	Exon9	c.1853 T > A	SNV
			P10	Exon2	c.304 A > T	SNV
4	FGF14	NM_001321937	P1	Exon4	c.424-3delT	Splicing
			P3	Exon4	c.424-3delT	Splicing
5	HSP90AA1	NM_005348	P2	Exon5	c.836_838delAGA	Deletion
			P3	Exon5	c.836_838delAGA	Deletion
6	KAT6A	NM_006766	P1	Exon2	c.282 A > T	SNV
			P2	Exon16	c.3218_3219insGGA	Insertion
7	KMT2D	NM_003482	P2	Exon13	c.4059_4061delGGA	Deletion
			P5	Exon10	c.1301 T > G	SNV
8	MAP3K1	NM_005921	P1	Exon14	c.2917_2918insCTC	Insertion
			P3	Exon20	c.4487delG	Deletion
9	RANBP2	NM_006267	P5	Exon16	c.2275 G > A	SNV
			P8	Exon20	c.6680 A > G	SNV
10	ZNF217	NM_006526	P1	Exon3	c.1645 G > A	SNV
			P10	Exon3	c.1645 G > A	SNV

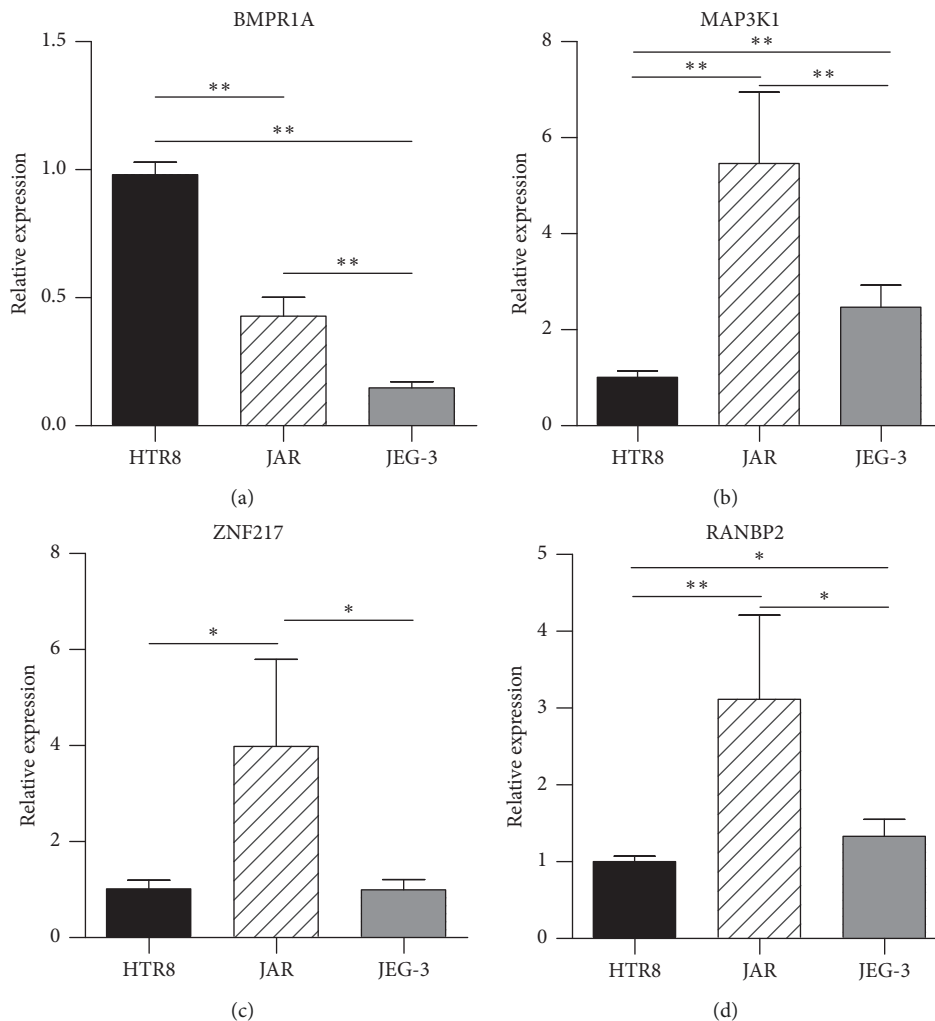


FIGURE 3: Continued.

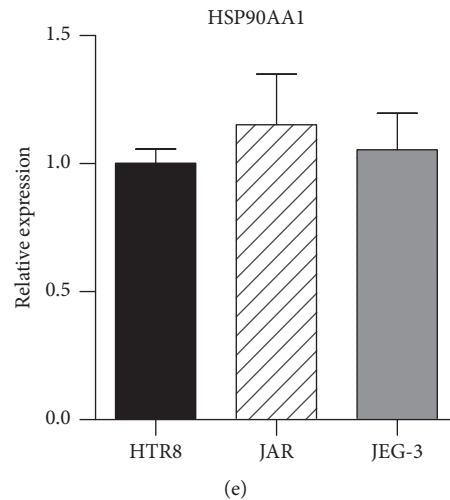


FIGURE 3: mRNA expression of mutations in cell lines (* $p < 0.05$, ** $p < 0.001$).

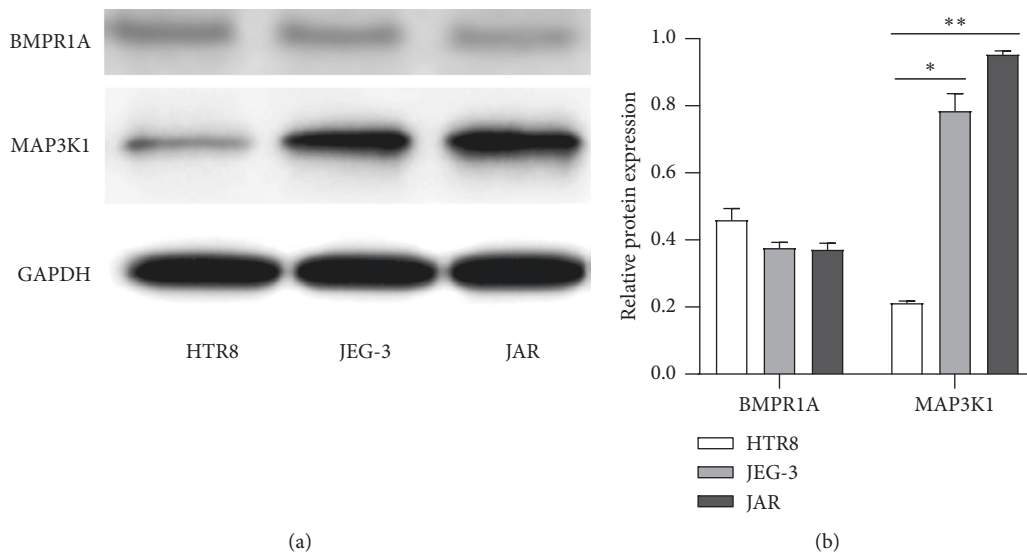


FIGURE 4: Protein expression of BMPR1A and MAP3K1 in three cell lines. (a) Western blotting gel image for BMPR1A and MAP3K1, and GAPDH was used as loading control. (b) Values of mean \pm S.D. of triplicate experiments were plotted (* $p < 0.05$, ** $p < 0.001$).

homolog (PTEN) and PI3K/Akt signaling pathways in patients with GTN. Gene ontology (GO) enrichment analysis provided support for positive regulation of several molecular functions, including regulation of DNA metabolic processes, regulation of hemopoiesis, and myeloid cell differentiation. Moreover, pathway enrichment analysis using the Kyoto Encyclopedia of Genes and Genomes (KEGG) database suggested the potential involvement of the PI3K/AKT signaling pathway, hepatocellular carcinoma, signaling pathways regulating pluripotency of stem cells, and extracellular signal-regulated kinase (ERK) 1 and ERK2 cascades.

Among the 11 patients with GTN evaluated in this study, *BMPR1A* mutations were detected in three patients (c.1001 T > C:p.L334S; 3/11, 27.3%). Interestingly, all three patients had lung metastases. Diseases associated with the protein coding gene *BMPR1A* include juvenile polyposis

syndrome and polyposis syndrome [24], and this gene has been shown to be related to the mammalian target of rapamycin (mTOR) and PI3K/AKT signaling pathways [25]. Low expression of *BMPR1A* also blocks the progression and metastasis of breast cancer [26], and *BMPR1A* may play a role in promoting the metastasis of GTN. GTN mainly spreads by hematogenous dissemination, with the lungs being the most common distant organ for GTN metastasis. According to GO enrichment analysis, regulation of hemopoiesis could play a role in the oncogenesis of GTN. Thus, tumor cells escape from the primary site and migrate into the circulatory system, and hematopoietic cells or cytokines may infiltrate tumor sites and generate a favorable microenvironment for tumor metastasis [27, 28]. Finally, the metastatic cells proliferate and form micrometastases or macrometastases.

Overall, our study demonstrated, for the first time, that cfDNA levels could have potential value in the assessment value in disease severity of GTN and that ctDNA sequencing may be a promising approach for identifying gene alterations in GTN. In the future, additional studies with more samples are needed to further explore the value of cfDNA sequencing in patients with GTN.

Data Availability

The data used to support the findings of this study are available from the corresponding author upon request.

Disclosure

Lingxiao Luo and Ling Lin are co-first authors.

Conflicts of Interest

The authors declare no conflicts of interest.

Authors' Contributions

Lingxiao Luo and Ling Lin contributed equally to this work. L. X. L. and L. L. were responsible for conceptualization, methodology, data analysis, and writing original draft preparation; X. Y. Z. and Q. Q. C. were responsible for conceptualization, investigation, and resources; H. B. Z. was responsible for visualization and software; and Q. C. and C. J. X. were involved in project administration, supervision, funding acquisition, and review and editing the manuscript.

Acknowledgments

This research was funded by Health Commission Project of Shanghai Municipality (no. 201344095) and the Natural Science Foundation of China (no. 81802766). We thank Dr. Xin Lu and Dr. Xiaoni Yue very much for scientific support.

Supplementary Materials

Supplementary Table 1. A targeted NGS panel including 559 genes. Supplementary Table 2. Normal distribution test for plasma HCG level. (*Supplementary Materials*)

References

- [1] M. J. Seckl, N. J. Sebire, and R. S. Berkowitz, "Gestational trophoblastic disease," *The Lancet*, vol. 376, no. 9742, pp. 717–729, 2010.
- [2] A. Santaballa, Y. García, A. Herrero et al., "SEOM clinical guidelines in gestational trophoblastic disease (2017)," *Clinical and Translational Oncology*, vol. 20, no. 1, pp. 38–46, 2018.
- [3] J. R. Lurain, "Gestational trophoblastic disease I: epidemiology, pathology, clinical presentation and diagnosis of gestational trophoblastic disease, and management of hydatidiform mole," *American Journal of Obstetrics and Gynecology*, vol. 203, no. 6, pp. 531–539, 2010.
- [4] J. T. Soper, D. G. Mutch, J. C. Schink, and A. C. O. Gynecologi, "Diagnosis and treatment of gestational trophoblastic disease: ACOG practice bulletin no. 53," *Gynecologic Oncology*, vol. 93, no. 3, pp. 575–585, 2004.
- [5] H. Y. S. Ngan, M. J. Seckl, R. S. Berkowitz et al., "Update on the diagnosis and management of gestational trophoblastic disease," *International Journal of Gynecology & Obstetrics*, vol. 143, pp. 79–85, 2018.
- [6] G. De Rubis, S. Rajeev Krishnan, and M. Bebawy, "Liquid biopsies in cancer diagnosis, monitoring, and prognosis," *Trends in Pharmacological Sciences*, vol. 40, no. 3, pp. 172–186, 2019.
- [7] C. Bettgowda, M. Sausen, R. J. Leary et al., "Detection of circulating tumor DNA in early- and late-stage human malignancies," *Science Translational Medicine*, vol. 6, no. 224, 2014.
- [8] I. Garcia-Murillas, G. Schiavon, B. Weigelt et al., "Mutation tracking in circulating tumor DNA predicts relapse in early breast cancer," *Science Translational Medicine*, vol. 7, no. 302, 2015.
- [9] J. Tie, I. Kinde, Y. Wang et al., "Circulating tumor DNA as an early marker of therapeutic response in patients with metastatic colorectal cancer," *Annals of Oncology*, vol. 26, no. 8, pp. 1715–1722, 2015.
- [10] G. Vandekerkhove, W. J. Struss, M. Annala et al., "Circulating tumor DNA abundance and potential utility in de novo metastatic prostate cancer," *European Urology*, vol. 75, no. 4, pp. 667–675, 2019.
- [11] Y. Wang, C. Zhao, L. Chang et al., "Circulating tumor DNA analyses predict progressive disease and indicate trastuzumab-resistant mechanism in advanced gastric cancer," *EBioMedicine*, vol. 43, pp. 261–269, 2019.
- [12] F. O. Committee, "FIGO staging for gestational trophoblastic neoplasia 2000. FIGO Oncology Committee," *International Journal of Gynaecology and Obstetrics: The Official Organ of the International Federation of Gynaecology and Obstetrics*, vol. 77, no. 3, pp. 285–287, 2002.
- [13] A. R. Thierry, S. El Messaoudi, P. B. Gahan, P. Anker, and M. Stroun, "Origins, structures, and functions of circulating DNA in oncology," *Cancer and Metastasis Reviews*, vol. 35, no. 3, pp. 347–376, 2016.
- [14] J. Uchida, K. Kato, Y. Kukita et al., "Diagnostic accuracy of noninvasive genotyping of EGFR in lung cancer patients by deep sequencing of plasma cell-free DNA," *Clinical Chemistry*, vol. 61, no. 9, pp. 1191–1196, 2015.
- [15] R. B. Corcoran and B. A. Chabner, "Application of cell-free DNA analysis to cancer treatment," *New England Journal of Medicine*, vol. 379, no. 18, pp. 1754–1765, 2018.
- [16] J. H. Strickler, J. M. Loree, L. G. Ahronian et al., "Genomic landscape of cell-free DNA in patients with colorectal cancer," *Cancer Discovery*, vol. 8, no. 2, pp. 164–173, 2018.
- [17] O. A. Zill, K. C. Banks, S. R. Fairclough et al., "The landscape of actionable genomic alterations in cell-free circulating tumor DNA from 21,807 advanced cancer patients," *Clinical Cancer Research*, vol. 24, no. 15, pp. 3528–3538, 2018.
- [18] M. R. Openshaw, R. A. Harvey, N. J. Sebire et al., "Circulating cell free DNA in the diagnosis of trophoblastic tumors," *EBioMedicine*, vol. 4, pp. 146–152, 2016.
- [19] W. Y. Pu, R. Zhang, L. Xiao et al., "Prediction of cancer progression in a group of 73 gastric cancer patients by circulating cell-free DNA," *BMC Cancer*, vol. 16, no. 1, p. 943, 2016.
- [20] N. Uehiro, F. Sato, F. Pu et al., "Circulating cell-free DNA-based epigenetic assay can detect early breast cancer," *Breast Cancer Research: BCR*, vol. 18, no. 1, p. 129, 2016.
- [21] G. R. Oxnard, C. P. Paweletz, and L. M. Sholl, "Genomic analysis of plasma cell-free DNA in patients with cancer," *JAMA Oncology*, vol. 3, no. 6, pp. 740–741, 2017.

- [22] Y. Sekiya, E. Yamamoto, K. Niimi et al., “c-Rel promotes invasion of choriocarcinoma cells via PI3K/AKT signaling,” *Oncology*, vol. 92, no. 5, pp. 299–310, 2017.
- [23] J. B. H. d. Mello, P. D. Ramos Cirilo, O. C. Michelin et al., “Genomic profile in gestational and non-gestational choriocarcinomas,” *Placenta*, vol. 50, pp. 8–15, 2017.
- [24] W. Cichy, B. Klincewicz, and A. Plawski, “State of the art paper Juvenile polyposis syndrome,” *Archives of Medical Science*, vol. 10, no. 3, pp. 570–577, 2014.
- [25] J. Lim, Y. Shi, C. M. Karner et al., “Dual function of Bmpr1a signaling in restricting preosteoblast proliferation and stimulating osteoblast activity in mouse,” *Development*, vol. 143, no. 2, pp. 339–347, 2016.
- [26] Y. Liu, R.-X. Zhang, W. Yuan et al., “Knockdown of bone morphogenetic proteins type 1a receptor (BMPRIa) in breast cancer cells protects bone from breast cancer-induced osteolysis by suppressing RANKL expression,” *Cellular Physiology and Biochemistry*, vol. 45, no. 5, pp. 1759–1771, 2018.
- [27] E. C. Finger and A. J. Giaccia, “Hypoxia, inflammation, and the tumor microenvironment in metastatic disease,” *Cancer and Metastasis Reviews*, vol. 29, no. 2, pp. 285–293, 2010.
- [28] B.-Z. Qian, “Inflammation fires up cancer metastasis,” *Seminars in Cancer Biology*, vol. 47, pp. 170–176, 2017.



Hindawi

Submit your manuscripts at
www.hindawi.com

